

RESEARCH ARTICLE

Loss of ADAM9 expression impairs β 1 integrin endocytosis, focal adhesion formation and cancer cell migration

Kasper J. Mygind¹, Jeanette Schwarz¹, Pranshu Sahgal², Johanna Ivaska^{2,3} and Marie Kveiborg^{1,*}

ABSTRACT

The transmembrane protease ADAM9 is frequently upregulated in human cancers, and it promotes tumour progression in mice. *In vitro*, ADAM9 regulates cancer cell adhesion and migration by interacting with integrins. However, how ADAM9 modulates integrin functions is not known. We here show that ADAM9 knockdown increases β 1 integrin levels through mechanisms that are independent of its protease activity. In ADAM9-silenced cells, adhesion to collagen and fibronectin is reduced, suggesting an altered function of the accumulated integrins. Mechanistically, ADAM9 co-immunoprecipitates with β 1 integrin, and both internalization and subsequent degradation of β 1 integrin are significantly decreased in ADAM9-silenced cells, with no effect on β 1 integrin recycling. Accordingly, the formation of focal adhesions and actin stress fibres in ADAM9-silenced cells is altered, possibly explaining the reduction in cell adhesion and migration in these cells. Taken together, our data provide mechanistic insight into the ADAM9–integrin interaction, demonstrating that ADAM9 regulates β 1 integrin endocytosis. Moreover, our findings indicate that the reduced migration of ADAM9-silenced cells is, at least in part, caused by the accumulation and altered activity of β 1 integrin at the cell surface.

KEY WORDS: ADAM9, β 1 integrin, Endocytosis, Focal adhesion, Migration

INTRODUCTION

A disintegrin and metalloproteinase (ADAM)-9 plays an important role in cancer. It is upregulated in a number of different human cancers, such as adenocarcinomas of the breast and prostate and its expression level often correlates to disease status and/or patient prognosis (Grützmann et al., 2004; O'Shea et al., 2003; Tao et al., 2010; Zubel et al., 2009). Studies using mouse cancer models indicate a pro-tumorigenic role of ADAM9, supportive of tumour development and metastasis (Fritzsche et al., 2008; Peduto et al., 2005). *In vitro* studies have demonstrated a positive role for ADAM9 on tumour cell adhesion, migration and invasion (Micocci et al., 2013; Nath et al., 2000; Zhou et al., 2001); however, the underlying mechanisms for these ADAM9 functions remain elusive.

As the name implies, ADAM9 is a multifunctional protein. It is a proteolytically active member of the large family of transmembrane ADAMs, whose main function is to cleave a variety of membrane-

anchored substrates [e.g. growth factors synthesized as transmembrane pro forms that require ADAM-mediated ectodomain shedding to bind and activate cognate receptors in an auto- and/or paracrine manner (Weber and Saftig, 2012)]. Among known ADAM9 substrates are members of the epidermal growth factor receptor (EGFR) ligands (Izumi et al., 1998), the fibroblast growth factor receptor (FGFR)-2 (Chan et al., 2012) and several vascular proteins (Guaiquil et al., 2009).


In addition to its proteolytic function, ADAM9 can interact with cell surface integrins, presumably via its disintegrin domain (Zhou et al., 2001). Integrins are membrane-spanning heterodimers composed of an α - and a β -subunit, whose composition determines their ability to bind different extracellular matrix (ECM) components (Hood and Chesh, 2002; Hynes, 2002). For example, α 1 β 1 and α 2 β 1 integrins are major collagen receptors, while α 5 β 1 binds fibronectin. Six different integrin subunits have been reported to interact with ADAM9, including α 2 β 1, α 3 β 1, α 6 β 1, α 9 β 1, α 6 β 4 and α V β 5 (Karadag et al., 2006; Mazzocca et al., 2005; Nath et al., 2000; Zhou et al., 2001). While the exact function of these interactions is still unclear, they have been implicated in the adhesion and migration of several types of tumour cells (Cominetti et al., 2009; Jossion et al., 2011; Martin et al., 2015; Mazzocca et al., 2005; Micocci et al., 2013; Wang et al., 2016).

Indeed, cell adhesion and migration are regulated via integrin-mediated cell–ECM interactions, which triggers outside-in signalling and subsequent remodelling of the actin cytoskeleton, including the formation of focal adhesions and actin stress fibres (Pellegrin and Mellor, 2007; Shattil et al., 2010). While such integrin functions take place at the cell surface, integrins are continuously internalized via clathrin- or caveolin-dependent endocytosis, after which they may be sent for lysosomal degradation or recycled back to the plasma membrane (De Franceschi et al., 2015). Importantly, these integrin trafficking events serve to regulate the adhesive and migratory properties of tumour cells (Paul et al., 2015).

Given the importance of tumour cell adhesion and migration for cancer invasion and metastasis, it is critical to better understand how ADAM9, through modulation of integrin functions acts to regulate these cellular processes. To this end, we here took a loss-of-function approach where ADAM9 expression was knocked down by means of siRNA in the human prostate cancer cell line PC3 and the fibrosarcoma cell line HT1080. We show that loss of ADAM9 leads to increased cell surface β 1 integrin levels, but, somewhat counterintuitively, decreased adhesion and cell migration on collagen type I and fibronectin. Our data indicate that the effect of ADAM9 knockdown on β 1 integrin expression is not conferred by loss of its protease function, but rather a disrupted ADAM9–integrin interaction, which results in decreased internalization and degradation of β 1 integrin, as well as altered focal adhesion and stress fibre formation in ADAM9-silenced cells. Based on these findings, we suggest that ADAM9 is required for optimal β 1 integrin endocytosis and that ADAM9-deficiency leads to the

¹Biotech Research and Innovation Centre (BRIC), University of Copenhagen, Ole Maaløes Vej 5, 2200 Copenhagen N, Denmark. ²Turku Centre for Biotechnology, University of Turku, Turku 20520, Finland. ³Department of Biochemistry, University of Turku, Turku 20520, Finland.

*Author for correspondence (marie.kveiborg@sund.ku.dk)

 M.K., 0000-0002-1293-1019

accumulation of $\beta 1$ integrin at the cell surface and perturbed cell adhesion and migration.

RESULTS

ADAM9 knockdown reduces integrin-mediated cell adhesion and migration

The human prostate cancer cell line PC3 has been used extensively to study cell adhesion, spreading and migration (Miao et al., 2000). By using siRNA-mediated knockdown, PC3 cells were efficiently silenced for ADAM9 expression (Fig. 1A). ADAM9-silenced cells showed decreased adhesion to both collagen type I (henceforth

termed collagen) and fibronectin, as compared to control siRNA cells (Fig. 1B). Adhesion was significantly reduced at 60 min after plating, and the difference was still evident after 2 h. Thus, ADAM9 knockdown appears to have a general effect on the adhesive machinery. Decreased adhesion to collagen and fibronectin was also observed upon ADAM9 knockdown in HT1080 cells, strengthening the observations from PC3 cells (Fig. S1).

To investigate how integrins are affected by knockdown of ADAM9, we stimulated cells with Mn^{2+} (Fig. 1C). Mn^{2+} treatment triggers integrin activation (Ni et al., 1998), yet failed to rescue the adhesion defect in ADAM9-knockdown cells. Interestingly, Mn^{2+} treatment enhanced the adhesion to fibronectin, but had no statistically significant effect on adhesion to collagen, indicating that one or more collagen receptors are already activated, a possibility that has been recently suggested for some integrins (Lu et al., 2016).

Given the decreased adhesion of cells deprived of ADAM9, we next wanted to investigate how cell spreading and migration are affected. Silencing ADAM9 significantly reduced spreading on both collagen and fibronectin (Fig. 1D,E). Moreover, migration of ADAM9-silenced PC3 cells was statistically significantly reduced (Fig. 1F,G). Thus, our findings support previous reports on the role of ADAM9 in integrin-mediated cell migration (Wang et al., 2016; Zhou et al., 2001).

ADAM9 knockdown leads to increased levels of $\beta 1$ integrin

To gain insight into the effect of ADAM9 knockdown on integrin function, we first examined the cell-surface expression of the two main β integrin subunits ($\beta 1$ and $\beta 3$ integrins) by flow cytometry. Confirming previous findings (Jossion et al., 2011), the level of $\beta 1$ integrin was upregulated almost 2-fold in both PC3 and HT1080 cells, whereas $\beta 3$ integrin was not statistically significantly altered (Fig. 2A,B). Total protein expression of $\beta 1$ integrin was similarly upregulated in ADAM9-silenced cells (Fig. 2C,D). The effect of ADAM9 knockdown on $\beta 1$ integrin protein expression was confirmed by additional siRNAs targeting ADAM9 in both PC3 and HT1080 cells (Fig. S2A–D). To determine whether the increased expression of $\beta 1$ integrin was a result of increased gene expression, we examined its mRNA (*ITGB1*) levels by qPCR (Fig. S2E–H). In PC3 cells, we found a 0.2-fold increase in steady-state $\beta 1$ integrin mRNA levels, while no changes were observed in HT1080 cells. Thus, the increased $\beta 1$ integrin protein levels are presumably not linked to increased transcription.

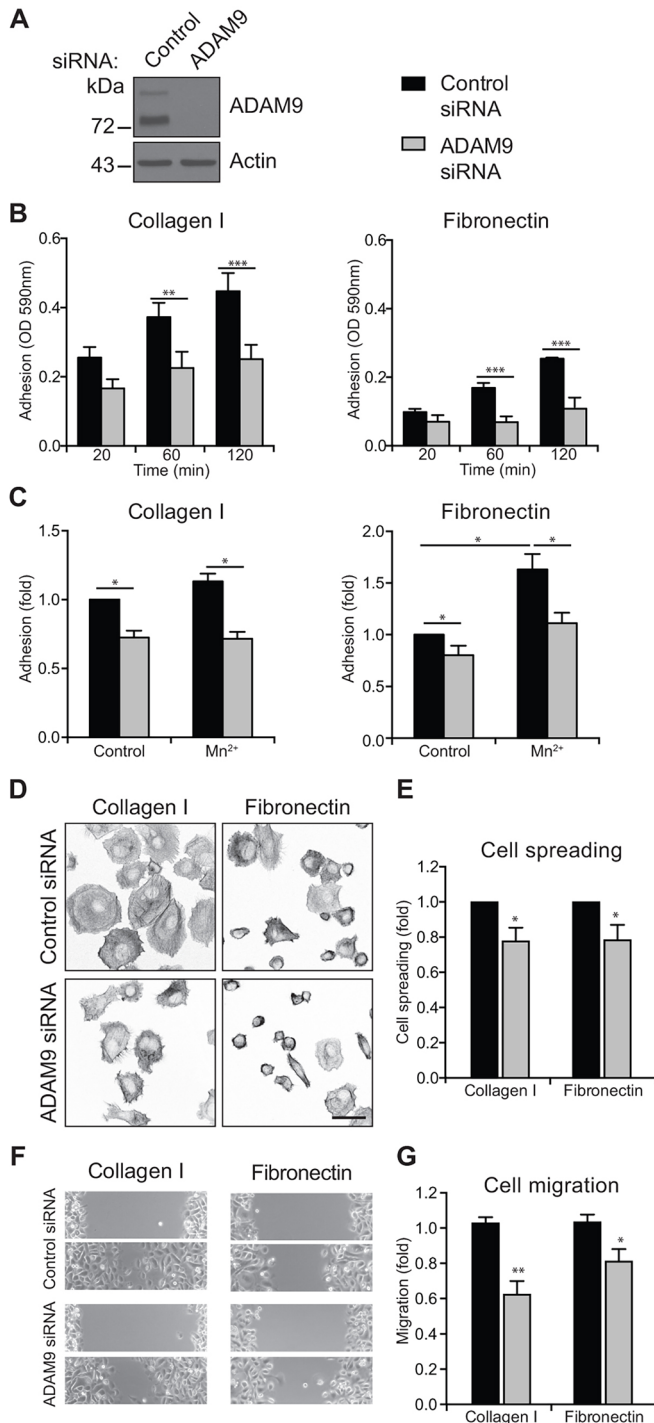


Fig. 1. ADAM9 knockdown reduces integrin-mediated cell adhesion and migration. PC3 cells were transfected with control or ADAM9 siRNA and incubated for 72 h. (A) Cells were lysed and examined by western blotting, using actin as a loading control. (B) Cells were plated on collagen I or fibronectin for 20, 60 or 120 min, and cell adhesion was measured colorimetrically. Adhesion to bovine serum albumin (BSA) was used as a control and was subtracted from the raw optical density (OD) values, $n=4$. (C) Prior to plating, cells were treated with or without 1 mM Mn^{2+} . Cells were then allowed to attach for 60 min and adhesion was determined as in B and calculated relative to untreated control cells, $n=3$. (D) Cells were plated on collagen I or fibronectin for 60 min, unbound cells were washed off, and attached cells were fixed in paraformaldehyde (PFA) and stained with phalloidin–Alexa–Fluor–488. Scale bar: 20 μm . (E) Cell spreading on collagen I and fibronectin quantified by determining the cell area using Image J and calculated relative to that in control-transfected cells, $n=4$. (F) Cells were plated on collagen I or fibronectin overnight. A p200 pipette tip was used to make a scratch wound and cells were left to migrate in medium with 2% FBS for 5 h. Migration distance was measured at 0 and 5 h. (G) Migration distance was quantified relative to control treated cells, which were set to 1, $n=4$. For all graphs, data are shown as mean \pm s.e.m. * $P < 0.05$, ** $P < 0.01$, *** $P < 0.005$ (Student's *t*-test or ANOVA when comparing two or multiple values, respectively).

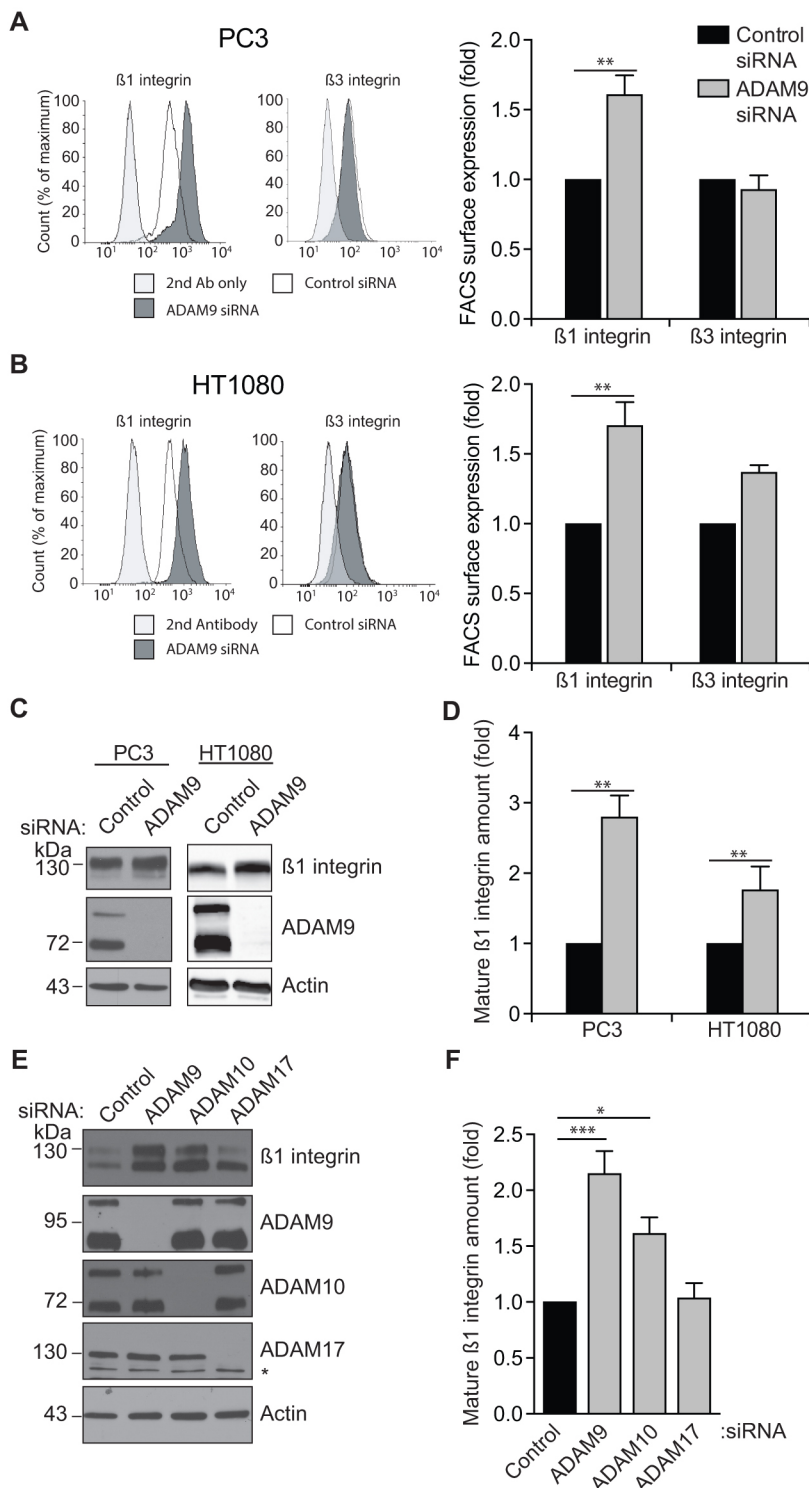


Fig. 2. ADAM9 knockdown leads to increased levels of $\beta 1$ integrin. PC3 and HT1080 cells were transfected with control or ADAM9 siRNA and 72 h later examined by (A,B) flow cytometry for surface expression of $\beta 1$ and $\beta 3$ integrin, or (C,D) western blotting, using actin as a loading control. (E) Cells were transfected with control or ADAM9, ADAM10 or ADAM17 siRNA, and 72 h later examined by western blotting. (F) Quantification of mature $\beta 1$ integrin (130 kDa band) from western blots as shown in E. For all graphs, data are shown as mean \pm s.e.m., $n=4$. * $P<0.05$, ** $P<0.01$, *** $P<0.005$ (ANOVA).

To further consolidate our findings, siRNA-resistant murine GFP-tagged ADAM9 was transiently expressed in cells with endogenous ADAM9 knocked down. However, although there was a tendency towards rescued $\beta 1$ integrin levels, the effect was not statistically significant (Fig. S3A,B). Next, to determine whether the effect on $\beta 1$ integrin is ADAM9 specific, we treated cells with siRNAs against ADAM9, ADAM10 and ADAM17 and analysed the protein expression of mature $\beta 1$ integrin. Fig. 2E,F shows that knockdown of ADAM9 and ADAM10 both increase the expression

of $\beta 1$ integrin, with ADAM9 having the most pronounced effect. In contrast, ADAM17 knockdown had no effect on the expression of $\beta 1$ integrin, thereby indicating some degree of protease specificity.

ADAM9 catalytic activity is dispensable for the regulation of $\beta 1$ integrin

Since ADAM9 knockdown results in an elevated level of $\beta 1$ integrin, we asked whether this effect involves the catalytic activity of ADAM9. To answer this question, we used the two broad

metalloproteinase inhibitors, GM6001 and Batimastat, to inhibit the catalytic activity of ADAM9 (Moss et al., 2010). Treatment with neither of the two inhibitors mimicked the increase in $\beta 1$ integrin observed when knocking down ADAM9 (Fig. 3A,B), indicating that the ADAM9 catalytic activity is dispensable for this effect. In addition, we tested whether the increase in $\beta 1$ integrin could be mediated by treating parental PC3 cells with conditioned medium from ADAM9-knockdown cells. As before, the expression of $\beta 1$ integrin was increased in ADAM9-silenced cells; yet, no effect was seen in cells grown in conditioned media from ADAM9-silenced cells (Fig. 3C,D).

To further test the implication of the catalytic activity of ADAM9, we examined migration on collagen in cells treated with GM6001 and Batimastat. In control siRNA-transfected cells, blocking metalloproteinase activity had a small, but not statistically significant, effect on cell migration, which did not mimic the effect of knocking down ADAM9 expression (Fig. 3E). Taken together, our findings indicate that ADAM9 regulates both $\beta 1$ integrin expression and $\beta 1$ integrin-mediated migration through mechanisms independent of its protease activity.

ADAM9 associates with internalized $\beta 1$ integrin

ADAM9 has been previously shown to interact with $\beta 1$ integrins (Mazzocca et al., 2005). To investigate the potential role of an ADAM9- $\beta 1$ -integrin interaction, we performed co-immunoprecipitation experiments. As shown in Fig. 4A, we found

an association between endogenous $\beta 1$ integrin and transiently expressed ADAM9-GFP in HT1080 cells. In addition, ADAM9-GFP was found to co-immunoprecipitate with a closed inactive conformation of $\beta 1$ integrin (Fig. 4B), which constitutes a substantial fraction of $\beta 1$ integrins at the cell surface (Arjonen et al., 2012).

The integrin-binding capacity of ADAM9 is presumably mediated via the extracellular disintegrin domain (Lu et al., 2007; Mahimkar et al., 2005). Thus, we tested the effect of mutating the ECD motif in the disintegrin domain, resembling the classical RGD integrin-binding motif (Anthis and Campbell, 2011) (Fig. S4). Notably, mutating the glutamic acid and cysteine residues in this motif (ADAM9-GA) severely affected the maturation of ADAM9 and consequently only a small amount of protein was detected in cell surface biotinylation experiments (Fig. S4A). Thus, the failure of the ADAM9-GA mutant to co-immunoprecipitate with $\beta 1$ integrin (Fig. S4B) is likely to be due to protein misfolding. Because of these findings, we generated another mutant (ADAM9-EG), which preserves the cysteine residue and therefore presumably does not interfere with disulphide bridges. However, since this mutation abolished maturation of ADAM9 even more severely (Fig. S4C), we could not determine the exact ADAM9 motif responsible for the association with $\beta 1$ integrin.

Interestingly, the co-immunoprecipitation experiments demonstrated that only the mature form of ADAM9 (~110 kDa in ADAM9-GFP) associates with $\beta 1$ integrin (Fig. 4A), indicating that this happens after pro-protein processing in the secretory pathway.

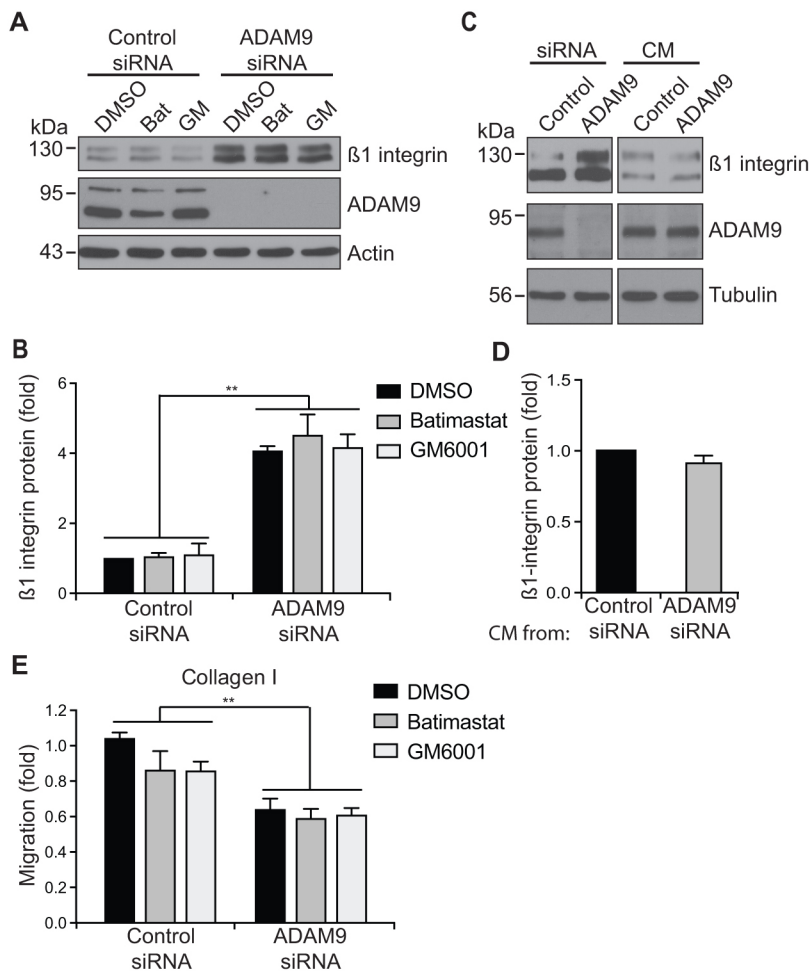


Fig. 3. ADAM9 catalytic activity is dispensable for the regulation of $\beta 1$ integrin.

(A) PC3 cells were transfected with control or ADAM9 siRNA. After 72 h, cells were treated with the broad-based metalloproteinase inhibitors Batimastat (Bat), GM6001 (GM), or vehicle control overnight and examined by western blotting as indicated. (B) Quantification of mature $\beta 1$ integrin normalized to the actin loading control from western blots as shown in A, $n=3$. (C) PC3 cells were transfected as in A, incubated for 72 h and then cultured in new medium for 24 h. Conditioned cell medium (CM) was then passed through a 0.2 μm filter and added to parental cells, which were incubated for an additional 24 h. Cell lysates were analysed by western blotting as indicated. (D) Quantification of mature $\beta 1$ integrin normalized to the tubulin loading control from western blots as shown in C, $n=3$. (E) PC3 cells transfected as in A were plated on collagen I overnight, scratch wounded with a p200 pipette tip, and left to migrate on collagen I in medium with 2% FBS and DMSO, GM6001 or Batimastat for 5 h, $n=4$. For all graphs, data are shown as mean \pm s.e.m. $**P<0.01$ (ANOVA).

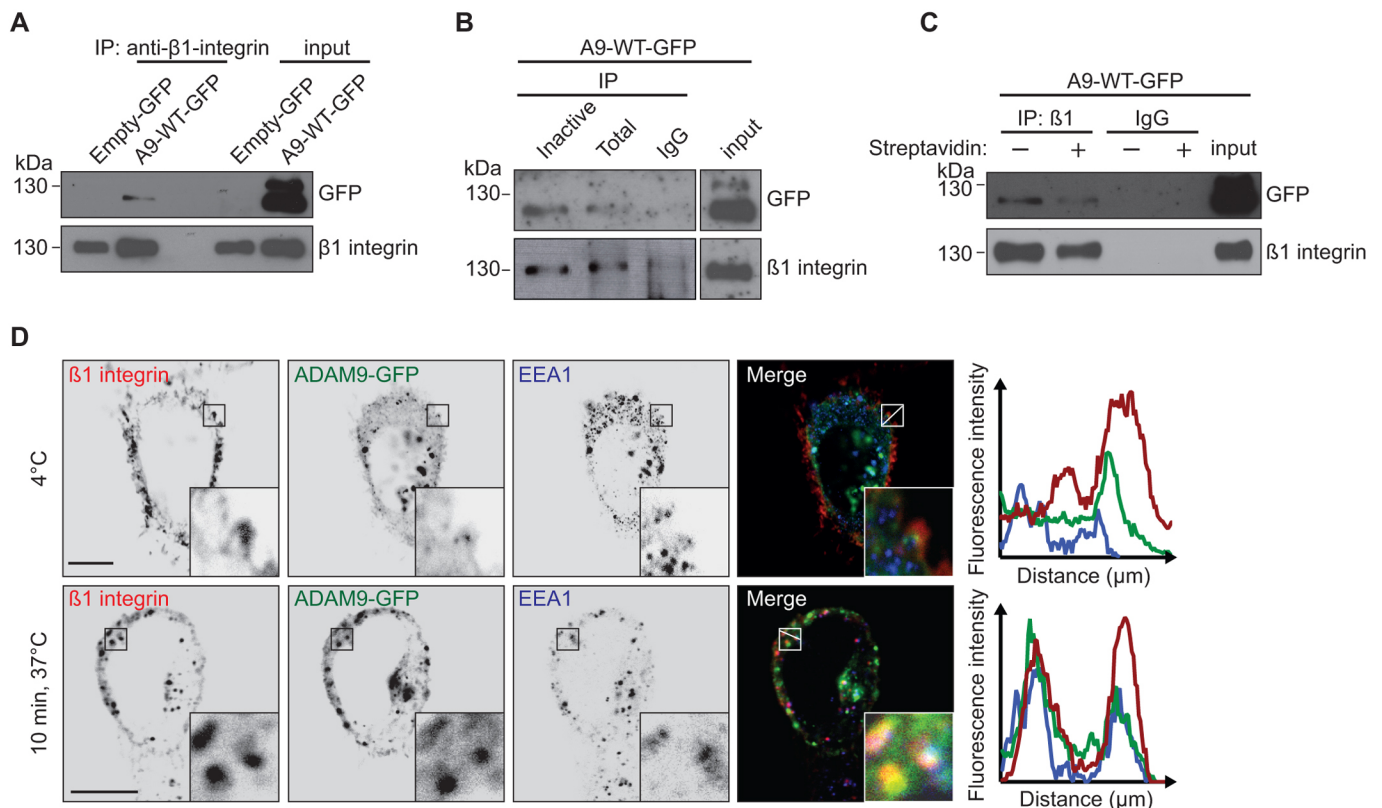


Fig. 4. ADAM9 associates with internalized $\beta 1$ integrin. (A) HT1080 cells were transfected with empty GFP vector (Empty-GFP) or wild-type ADAM9–GFP (A9-WT-GFP). Cells were lysed and immunoprecipitated (IP) with anti- $\beta 1$ integrin antibody. (B) HT1080 cells were transfected with wild-type ADAM9–GFP, lysed and immunoprecipitated with epitope-specific anti- $\beta 1$ integrin antibodies (inactive mAb13, total AB1952). (C) HT1080 cells were transfected with ADAM9–GFP and cell surface proteins were biotinylated. Cell lysates were divided into two, and left untreated or subjected to streptavidin pull-down (+) to clear the lysate of cell surface proteins. Both samples were immunoprecipitated with anti- $\beta 1$ integrin antibody and analysed by western blotting as indicated. (D) PC3 cells were transfected with ADAM9–GFP, and after 48 h cell surface $\beta 1$ integrins were labelled with antibody at 4°C, and the cells were fixed (4°C) or left to internalize for 10 min at 37°C and fixed (10 min, 37°C). Cells were subsequently permeabilized and stained for early endosome antigen 1 (EEA1), using appropriate fluorescently labelled secondary antibodies as indicated and examined by confocal microscopy. Fluorescence intensity were quantified along the line on the enlarged images (insets) and depicted on the graphs. Scale bars: 10 μ m. Single-channel images show inverted colours.

This led us to examine whether ADAM9 and $\beta 1$ integrin associate at the cell surface and/or intracellularly. To this end, we performed a cell surface removal assay. First, protein interactions were locked by dithiobis(succinimidyl propionate) (DSP) covalent linking, then cell surface proteins were deleted by biotin labelling and subsequent pull-down with streptavidin, and finally the depleted cell lysates were used for co-immunoprecipitation. While ADAM9– $\beta 1$ -integrin are expected to associate at the cell surface, there is also a small proportion in the intracellular fraction (Fig. 4C). Based on these data, we speculated that ADAM9 and $\beta 1$ integrin could associate on endocytic compartments. To test this, we examined the cellular localization of ADAM9 and $\beta 1$ integrin by immunofluorescence staining. Here, we expressed wild-type ADAM9–GFP in PC3 cells, and performed anti- $\beta 1$ integrin antibody uptake assays. As shown in Fig. 4D, we labelled cells kept at 4°C or allowed to internalize $\beta 1$ integrin by incubation at 37°C for 10 min with an anti- $\beta 1$ integrin antibody, and then fixed and stained the cells. Through confocal microscopy, we examined the potential colocalization with ADAM9–GFP, as well as whether their localization coincided on early endosomes (marked with EEA1). While little colocalization was seen in cells kept at 4°C, internalized $\beta 1$ integrin overlapped substantially with EEA1-positive endosomes and moreover, there was a partial colocalization with ADAM9–GFP (Fig. 4D).

ADAM9 is required for optimal $\beta 1$ integrin internalization

The potential association between ADAM9 and internalized $\beta 1$ integrin could indicate a role for ADAM9 in $\beta 1$ integrin endocytosis. To test this possibility, we labelled cell surface proteins with cleavable biotin and compared the internalization and recycling of $\beta 1$ integrin in control and ADAM9-silenced cells. Intriguingly, the internalization rate of $\beta 1$ integrin was markedly decreased in both PC3 (Fig. 5A) and HT1080 cells (Fig. 5B). In contrast, the recycling of internalized $\beta 1$ integrin back to the plasma membrane appears to be unaffected by ADAM9 knockdown, as shown by either examining the degree of internalization when inhibiting $\beta 1$ integrin recycling with Primaquine (Fig. 5C) or by directly monitoring the recycling of $\beta 1$ integrin (Fig. 5D).

With no effect on $\beta 1$ integrin recycling, the decreased internalization upon ADAM9 knockdown could result in decreased degradation and an overall net increase in $\beta 1$ integrin protein levels. To test this, we labelled surface proteins with non-cleavable biotin and incubated cells for up to 24 h to allow protein degradation. Remaining biotinylated proteins were detected by streptavidin pull-down and subsequent immunoblotting (Fig. 5E). Quantification of the amount of $\beta 1$ integrin left at different time points revealed a statistically significant increase in $\beta 1$ integrin protein stability in ADAM9-silenced cells (Fig. 5F), whereas the degradation rate of the transferrin receptor (TfR), which undergoes

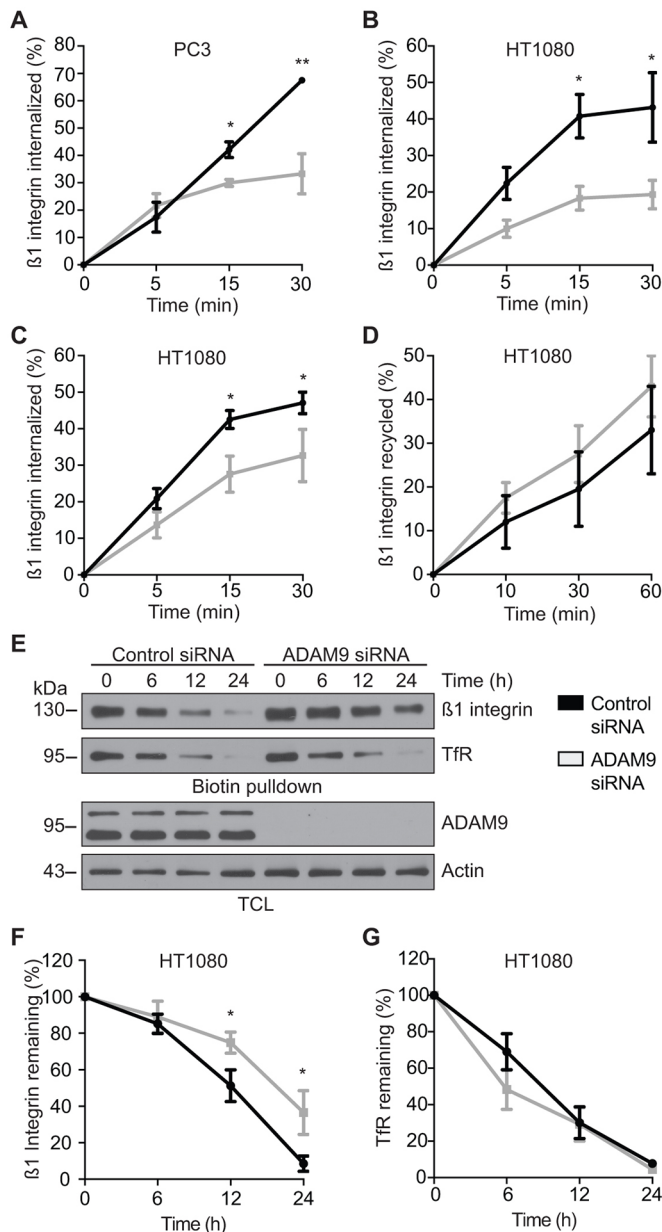


Fig. 5. ADAM9 is required for optimal $\beta 1$ integrin internalization. (A) PC3 cells were treated with control or ADAM9 siRNA and, 72 h later, $\beta 1$ integrin internalization was examined by labelling cell surface proteins with cleavable biotin at 4°C, followed by incubation at 37°C for the indicated time. Non-internalized biotin was removed from surface proteins by treating the cells with MesNa buffer. The amount of internalized $\beta 1$ integrin was determined by using Capture-ELISA. (B) An internalization assay using HT1080 cells was performed as described in A. (C) The internalization assay was performed as described in B, with the addition that cells were treated with 100 nM Primaquine (PQ) to inhibit recycling. (D) Recycling of $\beta 1$ integrin was largely done as described in B, with the exception that cells were incubated at 37°C for 30 min, then treated with MesNa buffer followed by a second incubation at 37°C to examine the recycling of $\beta 1$ integrin. (E) To examine the degradation of $\beta 1$ integrin, cell surface proteins were biotinylated, and cells were incubated at 37°C for the indicated time. Biotinylated proteins were precipitated using Streptavidin–agarose, and analysed by western blotting. The membrane was stripped and blotted for transferrin receptor (TfR) as an unaffected control. (F,G) The graphs show the quantification of $\beta 1$ integrin and TfR protein levels at the indicated time, respectively. The percentage protein at a given time was calculated relative to the initial amount of protein (0 h). For all graphs, data are shown as mean \pm s.e.m. For A–D, $n=3$ and for F–G, $n=4$. * $P<0.05$, ** $P<0.01$ (ANOVA).

similar constitutive endocytosis was unaffected (Fig. 5G). From this, we conclude that ADAM9 is important for the internalization of $\beta 1$ integrin and as a result, loss of ADAM9 expressions leads to accumulation of $\beta 1$ integrin at the cell surface.

ADAM9 knockdown leads to altered focal adhesion dynamics

Integrin endocytosis is a critical determinant of focal adhesion formation and turnover (Caswell and Norman, 2008). Therefore, we asked how loss of ADAM9 expression affects the formation of focal adhesions. To answer this question, we plated cells on collagen for 30, 60 and 360 min and stained for phosphorylated tyrosine residues (pTyr), which are highly enriched in early adhesion complexes (Parsons et al., 2010). Analysis of control siRNA-transfected cells by confocal microscopy revealed the formation of large mature adhesions 30 min after cell plating, which were even more pronounced and more centrally located after 60 min (Fig. 6A,B). In ADAM9-knockdown cells, the formation of pTyr-positive focal adhesions was noticeably delayed (Fig. 6B). After 6 h adhesion, the number of pTyr-positive complexes in control-transfected cells was clearly reduced, whereas at this time-point, the number and localization of pTyr-positive complexes in ADAM9-silenced cells resembled that for earlier time-points in control cells. This indicates that loss of ADAM9 slows down the maturation of focal adhesions, which was also shown by staining for paxillin phosphorylated at Y188 (pY118 paxillin), a mature focal adhesion marker (Parsons et al., 2010) (Fig. S5A,B). Extending the studies to focal adhesion turnover, live-cell internal reflection fluorescence (TIRF) microscopy showed that indeed, knockdown of ADAM9 reduced the focal adhesion turnover, quantified as the displacement of GFP-tagged vinculin in the cell for a period of 30 min (Fig. 6C–E).

Actin stress fibres are major cytoskeletal components linked to the plasma membrane at focal adhesions (Pellegrin and Mellor, 2007). Examining actin stress fibres by phalloidin staining, showed that in ADAM9-knockdown cell cultures, several cells showed a markedly altered pattern (Fig. 6F). In accordance with altered stress fibre formation, phosphorylation of cofilin-1 at serine 3 was increased (Fig. 6G), indicating a reduced actin-severing activity and consequently altered cytoskeletal remodelling (Ferraro et al., 2014).

ADAM9 regulates cell migration through modulation of $\beta 1$ integrin

Cell migration is highly regulated by integrin-dependent focal adhesion dynamics (Brakebusch and Fässler, 2005; Hood and Chersesh, 2002). Given the observed accumulation of $\beta 1$ integrin levels and altered focal adhesion dynamics in ADAM9-silenced cells, we asked whether these changes could explain the decrease in cell migration of said cells. To answer this question, we first analysed, by performing flow cytometry, the cell surface levels of two well-defined integrin α subunits, $\alpha 2$ and $\alpha 5$ integrins, which together with $\beta 1$ integrin constitute major collagen and fibronectin receptors, respectively. Here, the amount of $\alpha 2$ integrin on the cell surface was found to be upregulated, whereas the amount of $\alpha 5$ integrin was unaffected (Fig. 7A). Western blot analysis of total protein levels revealed a similar increase in $\alpha 2$ integrin, with no effect on $\alpha 5$ or αV integrin, upon ADAM9 knockdown (Fig. 7B,C). Moreover, the $\alpha 2$ integrin subunit was found to co-immunoprecipitate with GFP-tagged ADAM9, further indicating the importance of $\alpha 2\beta 1$ integrin (Fig. 7D).

We next tested whether the increased surface levels of the collagen-binding $\alpha 2\beta 1$ integrin contribute to the reduced migration of ADAM9-silenced cells on this substrate. By using an $\alpha 2\beta 1$

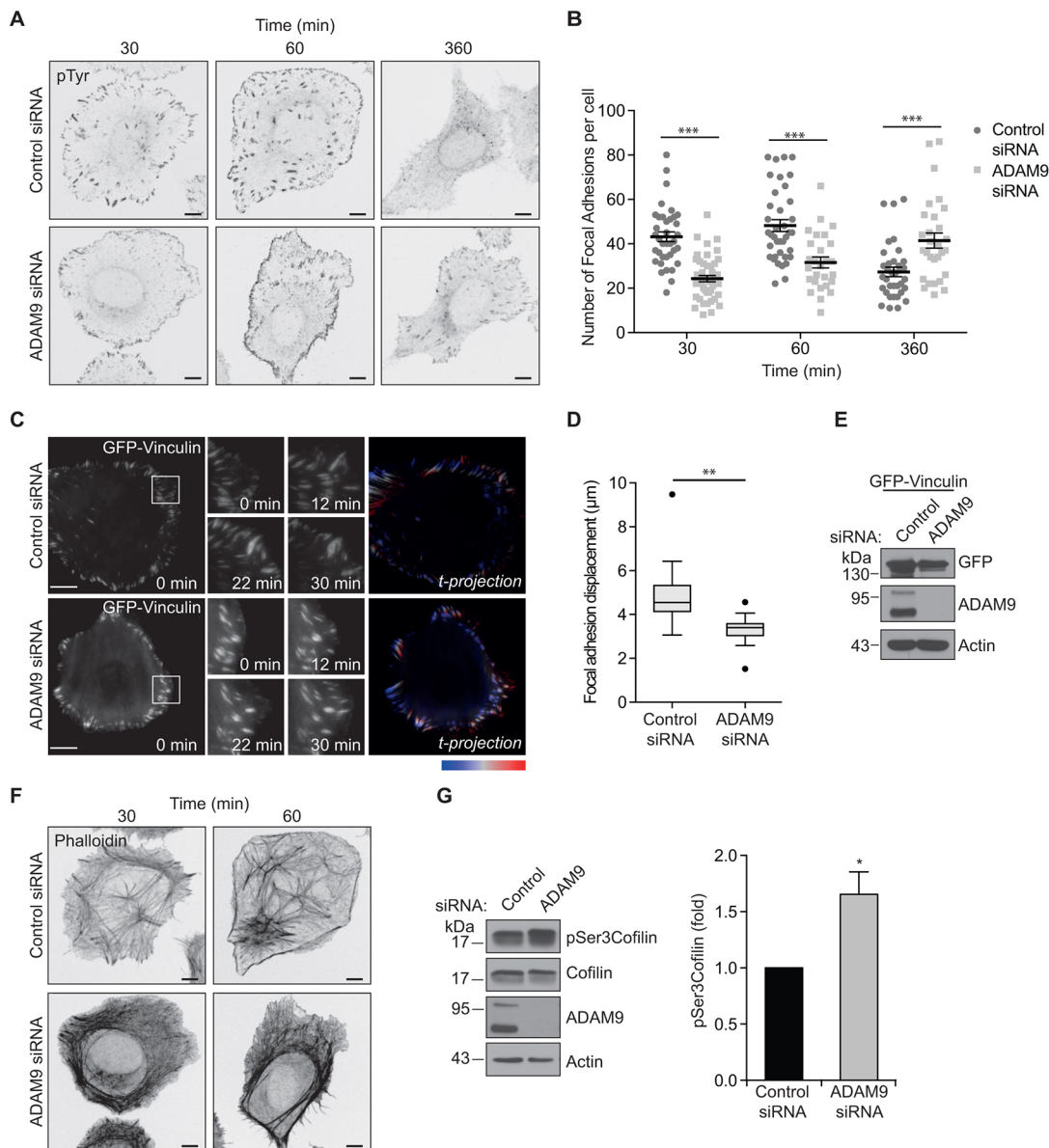


Fig. 6. ADAM9 knockdown leads to altered focal adhesion dynamics. (A) PC3 cells were transfected with control or ADAM9 siRNA. Cells were serum starved overnight and then plated on collagen for the indicated time. Cells were fixed and stained for phosphorylated tyrosine (pTyr), to detect focal adhesion complexes and examined by confocal microscopy. (B) Quantification of the number of large focal adhesions from experiments as shown in A (three independent experiments, 30 siControl and 46 siADAM9 cells analysed, and individual cells plotted; mean \pm s.e.m. values are indicated). (C) PC3 cells were transfected with control or ADAM9 siRNA. Cells were subsequently transfected with GFP–vinculin and plated on collagen. Cells were imaged live by using TIRF microscopy (one picture every 2 min for 30 min). (D) The length of focal adhesion displacement calculated in μ m (three independent experiments, 23 siControl and 21 siADAM9 videos analysed). The box represents the 25–75th percentiles, and the median is indicated. The whiskers show the s.e.m., and outliers are shown as dots. (E) Western blot showing knockdown of ADAM9 and expression of GFP–vinculin. (F) Same pictures as in A. Cells were stained for filamentous actin (phalloidin–Alexa-Fluor-488) and examined by confocal microscopy. Images in A and F are shown as inverted colours. (G) PC3 cells were treated with control or ADAM9 siRNA and after 72 h, cell lysates were analysed for pS3 cofilin-1 by western blotting. The quantification shown as mean \pm s.e.m., $n=3$. * $P<0.05$, ** $P<0.01$, *** $P<0.005$ (Student's *t*-test or ANOVA when comparing two or multiple values, respectively). Scale bars: 10 μ m (C) and 5 μ m (A,F).

integrin-specific inhibitory antibody (MAB1998z), we tested the effect of blocking $\alpha 2\beta 1$ integrins on the migration of PC3 cells. As shown in Fig. 7E, blocking $\alpha 2\beta 1$ integrin activity in control siRNA-transfected cells inhibited migration of cells plated on collagen. Cell migration on fibronectin served as a negative control, verifying that cell migration on this substrate is independent of $\alpha 2\beta 1$ integrin. As expected, ADAM9 knockdown inhibited cell migration on collagen; however, blocking $\alpha 2\beta 1$ integrin activity did not statistically significantly further inhibit migration in these cells

(Fig. 7E). Taken together, these findings suggest that loss of ADAM9 expression inhibits cell migration, at least in part through the accumulation of non-ligand-engaging $\beta 1$ integrins at the cell surface.

DISCUSSION

We here corroborate previous reports demonstrating that ADAM9 promotes cancer cell migration (Nath et al., 2000; Wang et al., 2016; Zhou et al., 2001). The effect of ADAM9 on migration has been

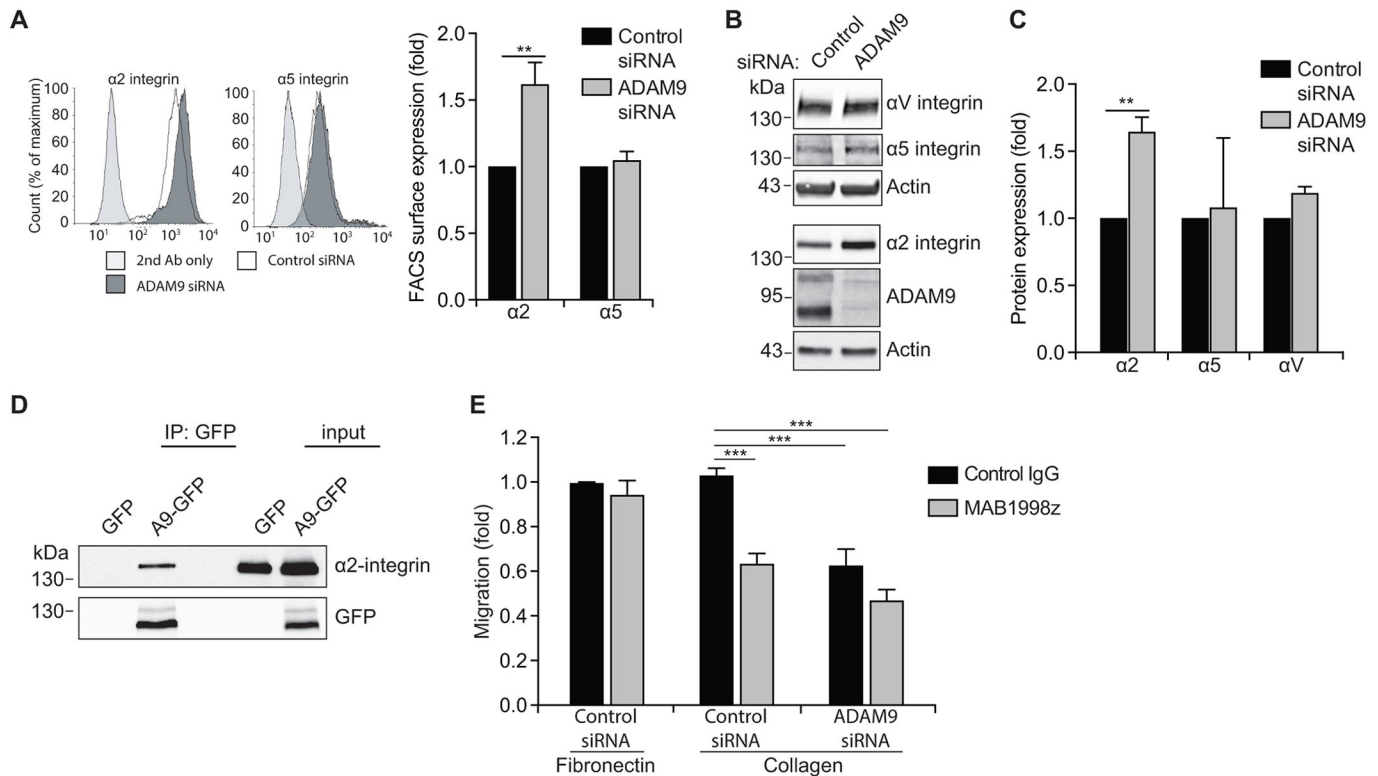


Fig. 7. ADAM9 regulates cell migration through modulation of $\beta 1$ integrin. (A,B) PC3 cells were transiently transfected with control or ADAM9 siRNA and, 72 h later, the levels of α integrin subunits were analysed by flow cytometry or western blotting, respectively. (C) The graph shows the quantification of integrin α subunits from western blots as shown in B, using actin as the loading control. (D) HT1080 cells were transfected with empty GFP vector (GFP) or wild-type ADAM9-GFP (A9-GFP). Cells were lysed, immunoprecipitated (IP) with anti-GFP antibody and examined by western blotting. (E) PC3 cells were transfected with control or ADAM9 siRNA and, 72 h later, cells were plated on fibronectin or collagen overnight and scratch wounded with a p200 pipette tip. Cells were then left to migrate in RPMI with 2% FBS with control IgG or MAB1998z, a $\alpha 2\beta 1$ integrin-specific inhibitory antibody, for 5 h. The data are shown as mean \pm s.e.m., $n=3$. ** $P<0.01$, *** $P<0.005$ (ANOVA).

suggested to involve the interaction of ADAM9 with cell surface integrin adhesion receptors (Mazzocca et al., 2005). However, exactly how ADAM9 affects integrin activity has, until now, not been clear. Using a loss-of-function approach, we here identified ADAM9 as a novel regulator of $\beta 1$ integrin endocytosis. Specifically, ADAM9 knockdown decreased $\beta 1$ integrin internalization, resulting in the accumulation of $\beta 1$ integrins at the cell surface. Serving as a proof of principle that the effect of ADAM9 on cell migration is, at least in part, due to perturbed integrin activity, blocking $\alpha 2\beta 1$ integrin collagen receptors failed to inhibit cell migration in ADAM9-depleted cells.

ADAM9 expression correlates with disease stage or patient prognosis in some human cancers (Fritzsche et al., 2008; Grützmann et al., 2004; Tao et al., 2010), and mouse models of, for example, prostate cancer have shown that ADAM9 acts to promote tumour progression (Peduto et al., 2005). Whether this is due to the ability of overexpressed ADAM9 to shed transmembrane substrates, such as epidermal growth factor (EGF) relies on non-proteolytic ADAM9 functions, or a combination of both is not clear. That said, the effect of ADAM9 on cancer cell adhesion and migration, shown in several reported *in vitro* studies and verified here, is likely to be an important contributor. Thus, understanding the molecular mechanisms whereby ADAM9 controls cancer cell migration is of great importance.

Cell migration is tightly regulated by cell surface integrin heterodimers, which bind the extracellular matrix to activate intracellular signalling pathways and induce actin cytoskeletal

remodelling (Shattil et al., 2010). We tested the effect of ADAM9 knockdown on the expression of two of the most important β subunits and found the surface expression of $\beta 1$ integrin, but not $\beta 3$ integrin, to be significantly upregulated as compared to what was seen in control cells. Increased $\beta 1$ integrin levels may seem contradictory to the observed decrease in cell adhesion, spreading and migration. However, the fact that stimulation of cells with Mn^{2+} was unable to fully increase cell adhesion in ADAM9-silenced cells, could indicate that the accumulated $\beta 1$ integrin is in a less active/more closed conformation or a less accessible localization. Indeed, we find that ADAM9 co-immunoprecipitates with the inactive (closed) form of $\beta 1$ integrin.

The increase in cell surface $\beta 1$ integrins reflected an increase in total cellular $\beta 1$ integrin, which could not be fully explained by increased $\beta 1$ integrin gene expression. Theoretically, the increase in $\beta 1$ integrin protein levels upon ADAM9 knockdown could be caused by loss of ADAM9 protease activity. For example, ADAM9 could shed $\beta 1$ integrin directly or another shed ADAM9 substrate could restrict $\beta 1$ integrin levels in an autocrine or paracrine manner. However, treating the cells with two broad-spectrum metalloproteinase inhibitors, one of which is known to inhibit ADAM9 protease activity (Cissé et al., 2005) did not mimic the effect of ADAM9 knockdown on either $\beta 1$ integrin levels or cell migration. Moreover, $\beta 1$ integrin levels were unaffected in parental cells cultured in conditioned medium from ADAM9-silenced cells, arguing against ADAM9 acting via paracrine signalling. Thus, while other ADAMs, such as ADAM17 have been shown to

increase cell migration by growth factor shedding (Maretzky et al., 2011), we suggest that ADAM9 regulates cell adhesion and migration by modulating the cell surface levels and activity of $\beta 1$ integrin in a protease-independent manner.

Since the catalytic activity of ADAM9 is dispensable for the regulation of $\beta 1$ integrin, we wanted to investigate whether the ADAM9– $\beta 1$ -integrin protein–protein interaction could be involved. Indeed, the extracellular disintegrin domain of ADAM9, and other ADAMs are similar to snake venom disintegrins that are well-known integrin antagonists (Takeda et al., 2012). While snake venom disintegrins bind integrins via a RGD motif in the so-called disintegrin loop, ADAM9 contains a structurally similar ECD motif (Lu et al., 2007) that has been shown to support the interaction with several different $\beta 1$ integrins, when used as a substrate in cell attachment assays (Zigrino et al., 2011). However, attempts at identifying the ADAM9– $\beta 1$ -integrin interaction motif were not successful, as mutation of the ADAM9 ECD motif prevented protein maturation (pro-protein processing).

Interestingly, however, only the mature form of ADAM9 was found to interact with $\beta 1$ integrin, suggesting that the interaction occurs after passage through the secretory pathway. Indeed, biotin-mediated removal of cell surface proteins followed by co-immunoprecipitation, together with confocal staining of ADAM9 and internalized $\beta 1$ integrin, indicate that ADAM9 interacts with $\beta 1$ integrin both at the cell surface and to a minor extent in early endosomal vesicles. Thus, while most previous reports studied the attachment of cells to recombinant extracellular ADAM9 fragments (Mazzocca et al., 2005), thereby reflecting an interaction between opposing cells (in trans), our data strongly indicate an association of ADAM9 and $\beta 1$ integrin in the same cell (in cis).

The continuous internalization and recycling of $\beta 1$ integrin is important for cell adhesion and migration (De Franceschi et al., 2015). Thus, the apparent interaction of ADAM9 with internalized $\beta 1$ integrin led us to examine the effect of ADAM9 on $\beta 1$ integrin endocytosis. By using biotin labelling and protein tracking assays, we showed that ADAM9 knockdown caused a statistically significant reduction in constitutive $\beta 1$ integrin internalization, and a subsequent delay in lysosomal degradation (Roberts et al., 2001). In contrast, $\beta 1$ integrin recycling was unaffected by ADAM9 knockdown. The identification of ADAM9 as a regulator of $\beta 1$ integrin endocytosis is a novel finding and the detailed mechanism whereby ADAM9 regulates the internalization of cell surface $\beta 1$ integrin has yet to be revealed. Interestingly, however, ADAM9 undergoes constitutive clathrin-dependent internalization with similar kinetics to $\beta 1$ integrin (unpublished data, K.J.M., Theresa Störko, Marie L. Freiberg, Jacob Samsoe-Petersen, J.S., Olav M. Andersen and M.K.), raising the possibility that the two proteins co-internalize. It is worth noting that ADAM9 has been previously shown to regulate the intracellular trafficking of E-cadherin (Hirao et al., 2006), whereas ADAM12 has been shown to co-internalize with TGF β receptor II (Atfi et al., 2007). Taken together, this could indicate a more general regulatory role for ADAM proteins in receptor endocytosis.

As with $\beta 1$ integrin endocytosis, several regulators have been identified. For example, sorting nexin 17 (SNX17) binds $\beta 1$ integrin on early endosomes and supports its recycling (Böttcher et al., 2012). More recently, the Golgi-localized γ -ear-containing Arf-binding (GGA)3 was shown to divert $\beta 1$ integrin from a degradative trafficking pathway, thereby supporting integrin stability, focal adhesion number and cell migration (Ratcliffe et al., 2016). Inspired by these findings, we investigated the effect of ADAM9 on the formation of focal adhesions, demonstrating a significant delay in

the maturation of focal adhesions in ADAM9-silenced cells. Maturation of focal adhesions requires force generation and relies on trafficking of endosomal integrins to the cell periphery (Gardel et al., 2010). Thus, defective integrin trafficking upon ADAM9 knockdown could result in defective bridging from ECM to the actin cytoskeleton. This could potentially also explain the altered appearance of actin stress fibres and the reduced activity of the actin-severing molecule cofilin-1 that we observed.

Cofilin-1 is a known downstream effector of the collagen receptor $\alpha 2\beta 1$ integrin (Ferraro et al., 2013). Well in line with the change in cofilin-1 activity, we found the $\alpha 2$ integrin subunit to be upregulated to the same degree as $\beta 1$ integrin. Thus, we hypothesize that ADAM9 knockdown results in reduced $\alpha 2\beta 1$ integrin internalization and accumulation of defective integrin heterodimers on the cell surface, ultimately leading to reduced cell adhesion and migration. To test this hypothesis, we blocked $\alpha 2\beta 1$ integrin activity by using a commercially available function-blocking antibody. Supporting our hypothesis, blocking $\alpha 2\beta 1$ integrin activity had a similar inhibitory effect on cell migration on collagen as did knockdown of ADAM9. In addition, blocking $\alpha 2\beta 1$ integrin in ADAM9-depleted cells failed to further inhibit cell migration, indicating that ADAM9 and $\alpha 2\beta 1$ integrins regulate cell migration through the same pathway. Surprisingly, no effects of ADAM9 on $\alpha 5$ or αV integrin levels were detected. Thus, additional studies are needed to identify the fibronectin receptor(s) responsible for the impaired cell adhesion and migration on this substrate.

In conclusion, we here describe a new regulatory mechanism, whereby ADAM9 controls the endocytosis of $\beta 1$ integrin. As such, loss of ADAM9 results in the accumulation of integrin at the cell surface, which fails to properly support the actin cytoskeletal remodelling and coupled migratory behaviours commonly induced by integrin-mediated outside-in signalling (Legate et al., 2009). Cell migration is crucial for the invasion and metastatic spread of cancer cells (Hood and Cheresch, 2002), and while the reported effects of ADAM9 on cancer cell invasion are somewhat controversial (Fry and Toker, 2010; Mazzocca et al., 2005; Wang et al., 2016), it will be important to investigate the implication of ADAM9-mediated integrin regulation in this context.

MATERIALS AND METHODS

Reagents and antibodies

The metalloproteinase inhibitors Batimastat (BB-94, 10 μ M) and GM6001 (Ilomastat, 10 μ M) were from Calbiochem and Sigma-Aldrich, respectively. HALT phosphatase inhibitor cocktail was from Thermo Fisher Scientific, and complete EDTA-free inhibitor cocktail was from Roche. Pure Col EZ was purchased from Advanced Biomatrix and human fibronectin was from Thermo Fisher. Primary antibodies used for western blotting, diluted 1:1000 unless otherwise stated, were against: $\alpha 2$ -integrin (BD Bioscience BD611017), $\alpha 5$ -integrin (Chemicon AB1949), αV -integrin (Abcam Ab124968), $\beta 1$ -integrin (OriGene EP1041Y, Millipore AB1952), $\beta 3$ -integrin (MCA728), ADAM9 (R&D Systems AF949), ADAM10 (Abcam Ab1997), ADAM17 (Abcam ab39162), Cofilin-1 (CST #5175), pS3 cofilin-1 (CST #3313), pTyr (Millipore 4G10), pY118 paxillin (CST #2541), GFP (Clontech #632592), Tfr (Invitrogen 13-6800), tubulin (Sigma T5168) and actin (Millipore Clone C4 MAB1501, 1:3000). Primary antibodies for immunoprecipitation were: GFP (Clontech #632592), $\beta 1$ -integrin (Millipore AB1952), inactive $\beta 1$ -integrin (mAb13 BD552828) and $\alpha 2$ integrin (MCA2025). Primary antibodies for flow cytometry and immunofluorescence staining used at 1:100 were against: $\alpha 2$ -integrin (MCA2025), $\alpha 5$ -integrin (MAB1999), $\beta 1$ -integrin (P5D2, AIIB2), and $\beta 3$ -integrin (MCA728), and purchased from Millipore and Bio Rad; EEA1 (Invitrogen F.43.1) was used at 1:200. Secondary rabbit horseradish peroxidase (HRP)-conjugated anti-goat-IgG antibody (P0449, 1:10,000) was from Dako, HRP-conjugated donkey anti-rabbit-IgG (NA934,

1:10,000) and sheep anti-mouse-IgG (NXA931, 1:10,000) antibodies were purchased from GE Healthcare. Secondary Alexa-Fluor-conjugated antibodies (A10036, A31571, A10040, A21434, 1:1000) and phalloidin-Alexa-Fluor-488 (A12379, 1:1500) were all from Invitrogen.

DNA constructs

Mammalian expression constructs encoding murine ADAM9-GFP in the pEGFP vector were kind gifts from William R. English and Gillian Murphy (Cambridge University, Cambridge, UK). The two disintegrin mutants of ADAM9-GFP were generated by mutating either amino acids 478 and 479 (ADAM9-GA mutant), or only residue 478 (ADAM9-EG mutant) in the conserved ECD motif to glutamic acid and alanine residues, respectively, using the QuickChange II Site-Directed Mutagenesis kit (Agilent Technologies #200521). The following primers were used for the GA mutant: forward (5'-AGAGGGAAGACCAATGGGTGTGATGTTCCCT-3'); reverse (5'-GCACATGGAGCCTCCTGGAAGGAAGTGGC-3'); and the EG mutant: forward (5'-AGAGGGAAGACCAAGTGGGTGTGATGTTCCCT-3'); reverse primer (5'-GCACATGGAGCCTCCTGGAAGGAAGTGGC-3').

Small interfering RNAs

Small interfering (si)RNAs targeting human ADAM9 (siGENOME #D004504-02 and -06), ADAM10 (siGENOME #D004503-01), and ADAM17 (SMARTpool #M-00345301) were purchased from Dharmacon. AllStars Negative Control siRNA (Qiagen #1027281) was used as a negative control in all siRNA transfections.

Cell culture

The human prostate cancer cell line PC3 and the human fibrosarcoma cell line HT1080 were both obtained from American Type Culture Collection (ATCC) and routinely tested for contamination. HT1080 cells were grown in Dulbecco's modified Eagle's medium (DMEM) (Gibco), whereas the PC3 cells were grown in RPMI medium (Gibco), and both media were supplemented with 10% fetal bovine serum (FBS) (HyClone). Cells were maintained at 37°C and in a 5% CO₂ humidified atmosphere. For live-cell imaging, cells were cultured in phenol-red free RPMI medium with glutamine, pyruvate, 25 mM HEPES and 2% FBS.

Transfections

Cells were grown to 40% confluence and transfected with siRNA by using Lipofectamine RNAiMAX (Invitrogen #13778). For 6 cm dishes, 16 pmol siRNA and 5 µl RNAiMAX were mixed with 300 µl optiMEM, incubated for 10 min at room temperature, and then added to the cells. Cells were incubated for 72 h. For transfection with plasmid DNA, cells were grown to 70–80% confluence in a six-well plate. 4 µl Lipofectamine 3000 (Invitrogen #11668) was mixed with 100 µl optiMEM and 2 µg DNA together with 4 µl Plus reagent were mixed with 100 µl optiMEM. Then 100 µl Lipofectamine solution was added to the DNA solution, mixed by a brief vortex, and incubated for 10 min at room temperature before adding to the cells. New medium was added the following day and cells were incubated for 24–48 h.

Conditioned medium

For the isolation of conditioned medium, cells were washed once with PBS and pre-warmed medium was added to the cells 48 h after transfection. After an additional 24 h incubation at 37°C, cell medium was isolated and filtered through a 0.45 µm filter (Sartorius #16555). Parental cells were washed once with PBS, the conditioned medium was added, and cells were incubated for 24 h at 37°C. Following incubation with conditioned medium, cells were analysed for integrin expression using western blotting.

Immunoprecipitations

HT1080 cells were transfected with tagged constructs as described above and incubated for 24–48 h. For immunoprecipitation (IP), cells were washed once with PBS at room temperature, then 10 mM DSP Crosslinker (Thermo Scientific #22585) diluted in DMSO-PBS was added to the cells and incubated for 30 min at RT. Cells were washed twice in PBS and lysed in ice-cold RIPA buffer (75 mM Tris-HCl pH 7.5, 150 mM NaCl, 0.1% SDS,

0.5% deoxycholate, 1 mM EDTA, 1% Triton X-100, Complete protease inhibitors (Roche). Lysates were cleared by centrifugation at 16,000 g for 10 min at 4°C and incubated with antibody overnight at 4°C. Pre-washed protein G-Sepharose beads were then added and further incubated for 1 h. The beads were washed three times with ice-cold lysis buffer, eluted in Laemmli reducing sample buffer, and the samples were boiled at 95°C for 10 min. Proteins were resolved by SDS-PAGE and analysed by western blotting.

SDS-PAGE and western blotting

Protein lysates were separated under denaturing conditions by SDS-PAGE (6–15% Acrylamide Tris-HCl, Bio-Rad) and transferred onto nitrocellulose membranes (Amersham 0.45 µm). Membranes were blocked in 5% milk or bovine serum albumin (BSA) in TBS-T for 1 h and incubated with primary antibody overnight at 4°C. Secondary horseradish peroxidase (HRP)-conjugated antibodies were incubated for 1 h at room temperature. Proteins were detected using ImageQuant LAS4000 and band intensities were determined by densitometric analysis using Total Lab. Blots shown are representative of at least three independent experiments.

Flow cytometry

Cells were washed once in PBS, detached by Trypsin treatment, and resuspended in complete growth medium. Cells were then pelleted by centrifugation at 2500 rpm for 3 min, and fixed by resuspension in 4% PFA-PBS solution for 10 min at room temperature. Cells were washed once in 1% BSA in PBS and incubated with primary antibody for 1 h at room temperature with rotation. After three washes, the cells were incubated with secondary antibody conjugated with Alexa-Fluor-488 or Alexa-Fluor-647 for 1 h at room temperature with rotation in the dark. Cells were washed three times and resuspended in 1% BSA in PBS and analysed by flow cytometry, using a FACSCalibur machine and analysed with FlowJo software.

Internalization assay

Cells were grown in complete growth medium in 6 cm dishes to 70–90% confluence. The cells were transferred to 4°C and washed twice with cold PBS. Cell surface proteins were labelled with 2 ml 0.05 mg/ml cleavable EZ-Link™ Sulfo-NHS-SS-Biotin (Pierce, Thermo Scientific #21331) in cold PBS for 30 min at 4°C. Unbound biotin was quenched off by washing three times with 100 mM glycine in cold PBS. Pre-warmed serum-free medium (SFM) was added to the cells (3 ml per dish) and biotin-labelled surface proteins were allowed to internalize at 37°C for varying time points. Internalization was stopped by transferring cells to 4°C and adding cold PBS to the dish. Surface biotin was removed by washing twice for 15 min in cold MesNa buffer [60 mM Sodium 2-mercaptoethanesulfonate (Sigma, 63705), 50 mM Tris pH 8.6, 100 mM NaCl, 1 mM EDTA, 0.2% BSA]. The total amount of surface biotinylation was detected by keeping a dish on ice after biotin labelling and omitting treatment with MesNa buffer. To verify proper removal of surface labelled biotin, a dish kept on ice after biotin labelling was washed three times with MesNa buffer. To block recycling, cells were pre-incubated with SFM containing 100 µM Primaquine or vehicle (DMSO) for 10 min at 4°C. For the internalization, Primaquine or vehicle were added to the pre-warmed medium. Recycling experiments were performed as described above with the exception that all samples were incubated for 30 min (internalization) and non-internalized biotin was removed by MesNa treatment. Cells were then incubated at 37°C again for the indicated time to let biotin-tagged protein recycle to the cell surface. Then cells were moved to 4°C and treated again with MesNa to remove biotin from recycled proteins. For Capture-ELISA analysis, cells were lysed [50 mM Tris-HCl pH 7.5, 100 mM NaCl, 1.5% Triton-X100, 0.5% NP-40, 7.5 mM EDTA, 7.5 mM EGTA and protease inhibitors (Roche Cocktail)]. Lysates were incubated for 30 min at 4°C on a spinning wheel prior to clearing at 16,400 g for 10 min.

Capture-ELISA

MaxiSorb 96-well plates were coated overnight with antibody (MAB1959, 1:500) in carbonate buffer (pH 9.6) at 4°C. Plates were washed once with PBS with 0.05% Tween-20 (PBS-T) and unspecific binding was blocked by incubation with 200 µl blocking buffer (5% BSA in PBS-T) for 1 h at room

temperature. 100 μ l of equalized cleared cell lysates were then incubated overnight at 4°C. Plates were washed 4 \times in PBS-T and incubated with Streptavidin-HRP (Pierce, #21130) in PBS-T with 1% BSA for 1 h at 4°C. Following washing with PBS-T five times, biotinylated proteins were detected by using TMB-Ultra (Thermo Scientific, #34028) peroxidase substrate. The reaction was stopped by adding 2 M sulphuric acid and absorbance was measured at 450 nm.

Immunofluorescence staining

Glass coverslips were coated with collagen I or fibronectin (10 μ g/ml) overnight at 37°C, and subsequently washed with PBS. Cells were serum starved overnight, washed once in PBS and detached using either HyQTase or Trypsin (peptidase function was stopped by adding SFM containing soya bean trypsin inhibitor). Cells were resuspended in SFM and seeded (20,000–100,000 cells/well) for the indicated time. For anti- β 1-integrin antibody uptake assays, cells were cultured on collagen-coated glass coverslips overnight, cooled on ice and surface labelled with antibody diluted in cold PBS. Unbound antibody was removed by washing twice in cold PBS. Cells were either kept on ice to prevent internalization or incubated in pre-warmed complete medium at 37°C for 10 min. Following incubation at 37°C, cells were washed with ice-cold PBS, and un-internalized antibody was removed by incubation with cold acetic acid buffer (0.5% acetic acid, 0.5 M NaCl, pH 3.0) for 2 min. Cells were washed once in PBS (room temperature), fixed in 4% PFA for 10 min (RT), and permeabilized in 0.2% Triton X-100 or Saponin for 10 min at room temperature. Free aldehyde groups were quenched by incubation with 0.1 M NH_4Cl in PBS for 10 min and blocked in either 2% BSA in PBS-T for 30 min followed by incubation with primary antibody overnight at 4°C. Secondary antibody diluted in blocking buffer containing phalloidin-Alexa-Fluor-488 was incubated for 1 h at room temperature in the dark. Images were collected by confocal microscopy (Leica SP8) with a \times 63/1.4 NA oil objective, by using Leica imaging software (Leica Application Suite X). Fluorescence intensity (line scan) was quantified along the line on the enlarged images and depicted on the graphs, using ImageJ.

Live-cell imaging

To analyse the dynamics of focal adhesions, cells were transfected with GFP-vinculin and plated for 1 h on collagen before live imaging on a TIRF microscope, at 37°C, in the presence of 5% CO_2 . Images were acquired every 2 min for 30 min, using a 100 \times (NA 1.46 oil, alpha Plan-Apochromat, DIC) objective. Acquired videos were processed with ImageJ; in particular the contrast was adjusted to equalize the fluorescence signal. To measure vinculin translocation, z-projections were made and ten trajectories of migration were measured and averaged to a single value for each cell measured. Cells were plated on Ibidi μ -Slide 8-well chambers (Nunc).

Adhesion assay

Cells were washed twice in PBS and serum-starved overnight by incubating in SFM. MaxiSorb 96-well plates were coated with collagen I, fibronectin or BSA (1–10 μ g/ml) overnight at 37°C and blocked with 0.1% BSA in PBS for 2 h at 37°C. Blocked 96-well plates were washed once with PBS prior to cell attachment. Cells were washed once in PBS, detached using Trypsin, and resuspended in SFM for 30 min, then seeded (20,000 cells/well) on the plates, and allowed to adhere for 20–120 min at 37°C. For Mn^{2+} stimulation, 1 mM Mn^{2+} were added to the cells in suspension 5 min prior to plating. Cells were allowed to adhere for 60 min. Cells were then washed gently twice with PBS, fixed with 4% PFA for 10 min at room temperature, washed three times with PBS, and cells were stained with 0.1% Crystal Violet (Sigma C6158) for 20 min. Plates were washed thoroughly with deionized water and then incubated with 1% SDS in PBS for 15 min. Adhesion was determined by colorimetric measurements at 600 nm.

Migration assay

The bottom of a 24-well plate was marked by making a thin horizontal line with a scalpel, then the wells were coated with collagen I and fibronectin in PBS, incubated at 37°C overnight. Cells were seeded overnight to reach 100% confluence. A vertical scratch wound was made with a p200 pipette tip. The medium was removed and the well was washed once in medium containing 2% FBS. The cells were then incubated in 2% FBS medium for

the indicated time. Pictures of the cells were taken at 0 and 5 h after scratch wound. Inhibitory antibodies or broad-spectrum metalloproteinase inhibitors (Batimastat and GM6001) were added to the medium.

Protein turnover

Cells were seeded in 6 cm dishes, grown to 80% confluence, transferred to 4°C, and washed twice with cold PBS. Cell surface proteins were labelled with 2 ml of 0.2 mg/ml non-cleavable EZ-Link™ Sulfo-NHS-LC-Biotin (Pierce, Thermo Scientific #21335) in cold PBS for 30 min at 4°C. Unbound biotin was quenched of by washing three times in 100 mM glycine in cold PBS. Pre-warmed complete medium was then added to the cells, which were incubated at 37°C for the indicated time, washed twice in cold PBS, and lysed in lysis buffer [50 mM Tris-HCl pH 7.5, 100 mM NaCl, 1.5% Triton-X100, 0.5% NP-40, 7.5 mM EDTA, 7.5 mM EGTA and protease inhibitors (Roche Cocktail)]. Lysates were incubated on a spinning wheel at 4°C for 30 min, cleared by centrifugation at 16,400 g for 10 min, and biotinylated proteins were pulled down using Streptavidin-agarose beads (Sigma S1638). Equal amounts of protein lysate were incubated with beads for 2 h at 4°C and washed three times in lysis buffer (diluted 1:3 in PBS). After the last wash, beads were sucked dry and 30 μ l 5 \times sample buffer with 100 mM dithiothreitol (DTT) was added. Samples were boiled at 95°C for 5 min, spun down at 16,400 g for 2 min, and analysed by SDS-PAGE followed by western blotting.

Quantitative PCR

Cells were cultured in six-well plates, washed twice in cold PBS, and RNA was isolated from cells by using an RNeasy mini kit (Qiagen #74104). cDNA was synthesized by using the iScript cDNA Synthesis kit (Bio-Rad #170-8890), according to manufacturer's protocol. Quantitative PCR was performed using SYBR Green (ThermoFisher #K0221), with the following primers: β 1 integrin-forward (5'-CGATGCCATCATGCAAGT-3'), β 1 integrin-reverse (5'-ACACCAGCAGCCGTGTAAC-3'), ADAM9-forward (5'-GACCCTTCGTGTCGGT-3'), ADAM9-reverse (5'-GAAAGATGTGAGGTCTGTTGAAAG-3'), Actin-forward (5'-TTCTACAATGAGCTGCGTGTG-3'), Actin-reverse (5'-GGGGTGTGTAAGGTCTCAA-3').

Statistics

All data are shown as the mean \pm s.e.m. of at least three independent experiments and were analysed by performing an unpaired Student's *t*-test or analysis of variance (ANOVA) with the Tukey's post-test as appropriate, using GraphPad Prism version 7 for Macintosh (GraphPad Software). In all cases, *P*<0.05 was considered statistically significant.

Acknowledgements

The authors thank William R. English and Gillian Murphy (Cambridge University, UK) for kindly providing the ADAM9 expression constructs. We thank the Core Facility for Integrated Microscopy, Faculty of Health and Medical Sciences, University of Copenhagen for their help with live-cell TIRF microscopy.

Competing interests

The authors declare no competing or financial interests.

Author contributions

Conceptualization: J.I., M.K.; Methodology: K.J.M., J.S.; Validation: P.S.; Formal analysis: K.J.M., M.K.; Investigation: K.J.M.; Data curation: K.J.M., M.K.; Writing - original draft: K.J.M.; Writing - review & editing: J.I., M.K.; Supervision: J.I., M.K.; Project administration: M.K.; Funding acquisition: J.I., M.K.

Funding

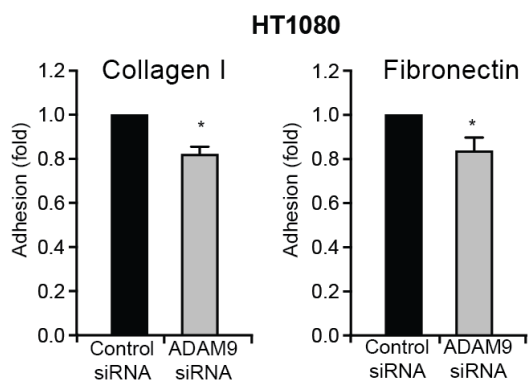
This study was funded by grants from The Lundbeck Foundation (Lundbeckfonden), The Danish Cancer Society (Kræftens Bekæmpelse), and Københavns Universitets Fond for Kræftforskning to M.K. K.J.M. was supported by a Ph.D. fellowship from the Faculty of Health and Medical Sciences, University of Copenhagen (Københavns Universitet). J.I. was supported by European Research Council (ERC) (CoG #615258) and the Academy of Finland. P.S. has been supported by Turku Doctoral program for Molecular Medicine (TuDMM).

Supplementary information

Supplementary information available online at <http://jcs.biologists.org/lookup/doi/10.1242/jcs.205393.supplemental>

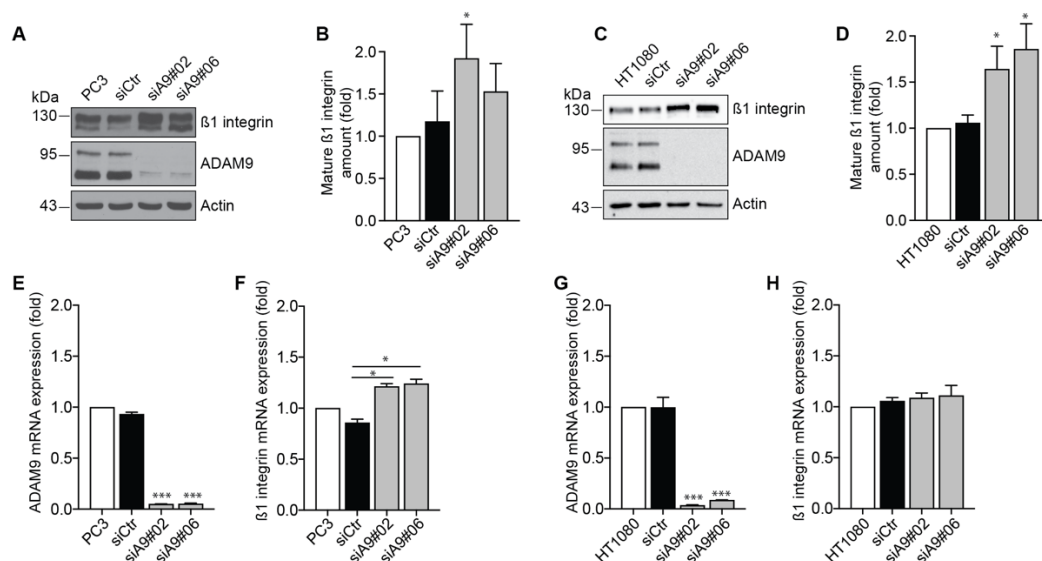
References

- Anthis, N. J. and Campbell, I. D. (2011). The tail of integrin activation. *Trends Biochem. Sci.* **36**, 191-198.
- Arjonen, A., Alanko, J., Veltel, S. and Ivaska, J. (2012). Distinct recycling of active and inactive beta1 integrins. *Traffic* **13**, 610-625.
- Atfi, A., Dumont, E., Colland, F., Bonnier, D., L'Helgoualc'h, A., Prunier, C., Ferrand, N., Clément, B., Wewer, U. M. and Thérêt, N. (2007). The disintegrin and metalloproteinase ADAM12 contributes to TGF-beta signaling through interaction with the type II receptor. *J. Cell Biol.* **178**, 201-208.
- Böttcher, R. T., Stremmel, C., Meves, A., Meyer, H., Widmaier, M., Tseng, H.-Y. and Fässler, R. (2012). Sorting nexin 17 prevents lysosomal degradation of beta1 integrins by binding to the beta1-integrin tail. *Nat. Cell Biol.* **14**, 584-592.
- Brakebusch, C. and Fässler, R. (2005). beta 1 integrin function in vivo: adhesion, migration and more. *Cancer Metastasis Rev.* **24**, 403-411.
- Caswell, P. and Norman, J. (2008). Endocytic transport of integrins during cell migration and invasion. *Trends Cell Biol.* **18**, 257-263.
- Chan, K. M., Wong, H. L. X., Jin, G., Liu, B., Cao, R., Cao, Y., Lehti, K., Tryggvason, K. and Zhou, Z. (2012). MT1-MMP inactivates ADAM9 to regulate FGFR2 signaling and calvarial osteogenesis. *Dev. Cell* **22**, 1176-1190.
- Cissé, M. A., Sunyach, C., Lefranc-Jullien, S., Postina, R., Vincent, B. and Checler, F. (2005). The disintegrin ADAM9 indirectly contributes to the physiological processing of cellular prion by modulating ADAM10 activity. *J. Biol. Chem.* **280**, 40624-40631.
- Cominetti, M. R., Martin, A. C. B. M., Ribeiro, J. U., Djaafri, I., Fauvel-Lafève, F., Crépin, M. and Selistre-de-Araujo, H. S. (2009). Inhibition of platelets and tumor cell adhesion by the disintegrin domain of human ADAM9 to collagen I under dynamic flow conditions. *Biochimie* **91**, 1045-1052.
- De Franceschi, N., Hamidi, H., Alanko, J., Sahgal, P. and Ivaska, J. (2015). Integrin traffic - the update. *J. Cell Sci.* **128**, 839-852.
- Ferraro, A., Mourtoukou, D., Kosmidou, V., Avlonitis, S., Kontogeorgos, G., Zografos, G. and Pintzas, A. (2013). EZH2 is regulated by ERK/AKT and targets integrin alpha2 gene to control Epithelial-Mesenchymal Transition and anoikis in colon cancer cells. *Int. J. Biochem. Cell Biol.* **45**, 243-254.
- Ferraro, A., Boni, T. and Pintzas, A. (2014). EZH2 regulates cofilin activity and colon cancer cell migration by targeting ITGA2 gene. *PLoS ONE* **9**, e115276.
- Fritzsche, F. R., Wassermann, K., Jung, M., Tölle, A., Kristiansen, I., Lein, M., Johannsen, M., Dietel, M., Jung, K. and Kristiansen, G. (2008). ADAM9 is highly expressed in renal cell cancer and is associated with tumour progression. *BMC Cancer* **8**, 179.
- Fry, J. L. and Toker, A. (2010). Secreted and membrane-bound isoforms of protease ADAM9 have opposing effects on breast cancer cell migration. *Cancer Res.* **70**, 8187-8198.
- Gardel, M. L., Schneider, I. C., Aratyn-Schaus, Y. and Waterman, C. M. (2010). Mechanical integration of actin and adhesion dynamics in cell migration. *Annu. Rev. Cell Dev. Biol.* **26**, 315-333.
- Grützmann, R., Lüttges, J., Sipos, B., Ammerpohl, O., Dobrowolski, F., Alldinger, I., Kersting, S., Ockert, D., Koch, R., Kalthoff, H. et al. (2004). ADAM9 expression in pancreatic cancer is associated with tumour type and is a prognostic factor in ductal adenocarcinoma. *Br. J. Cancer* **90**, 1053-1058.
- Guaquil, V., Swendeman, S., Yoshida, T., Chavala, S., Campochiaro, P. A. and Blobel, C. P. (2009). ADAM9 is involved in pathological retinal neovascularization. *Mol. Cell. Biol.* **29**, 2694-2703.
- Hirao, T., Nanba, D., Tanaka, M., Ishiguro, H., Kinugasa, Y., Doki, Y., Yano, M., Matsuura, N., Monden, M. and Higashiyama, S. (2006). Overexpression of ADAM9 enhances growth factor-mediated recycling of E-cadherin in human colon cancer cell line HT29 cells. *Exp. Cell Res.* **312**, 331-339.
- Hood, J. D. and Cheresch, D. A. (2002). Role of integrins in cell invasion and migration. *Nat. Rev. Cancer* **2**, 91-100.
- Hynes, R. O. (2002). Integrins: bidirectional, allosteric signaling machines. *Cell* **110**, 673-687.
- Izumi, Y., Hirata, M., Hasuwa, H., Iwamoto, R., Umata, T., Miyado, K., Tamai, Y., Kurisaki, T., Sehara-Fujisawa, A., Ohno, S. et al. (1998). A metalloprotease-disintegrin, MDC9/meltrin-gamma/ADAM9 and PKCdelta are involved in TPA-induced ectodomain shedding of membrane-anchored heparin-binding EGF-like growth factor. *EMBO J.* **17**, 7260-7272.
- Josson, S., Anderson, C. S., Sung, S.-Y., Johnstone, P. A. S., Kubo, H., Hsieh, C.-L., Arnold, R., Gururajan, M., Yates, C. and Chung, L. W. K. (2011). Inhibition of ADAM9 expression induces epithelial phenotypic alterations and sensitizes human prostate cancer cells to radiation and chemotherapy. *Prostate* **71**, 232-240.
- Karadag, A., Zhou, M. and Croucher, P. I. (2006). ADAM-9 (MDC-9/meltrin-gamma), a member of the a disintegrin and metalloproteinase family, regulates myeloma-cell-induced interleukin-6 production in osteoblasts by direct interaction with the alpha(v)beta5 integrin. *Blood* **107**, 3271-3278.
- Legate, K. R., Wickstrom, S. A. and Fässler, R. (2009). Genetic and cell biological analysis of integrin outside-in signaling. *Genes Dev.* **23**, 397-418.
- Lu, X., Lu, D., Scully, M. F. and Kakkar, V. V. (2007). Structure-activity relationship studies on ADAM protein-integrin interactions. *Cardiovasc. Hematol. Agents Med. Chem.* **5**, 29-42.
- Lu, Z., Mathew, S., Chen, J., Hadziselimovic, A., Palamuttam, R., Hudson, B. G., Fassler, R., Pozzi, A., Sanders, C. R. and Zent, R. (2016). Implications of the differing roles of the beta1 and beta3 transmembrane and cytoplasmic domains for integrin function. *Elife* **5**, e18633.
- Mahimkar, R. M., Visaya, O., Pollock, A. S. and Lovett, D. H. (2005). The disintegrin domain of ADAM9: a ligand for multiple beta1 renal integrins. *Biochem. J.* **385**, 461-468.
- Maretzky, T., Evers, A., Zhou, W., Swendeman, S. L., Wong, P.-M., Rafii, S., Reiss, K. and Blobel, C. P. (2011). Migration of growth factor-stimulated epithelial and endothelial cells depends on EGFR transactivation by ADAM17. *Nat. Commun.* **2**, 229.
- Martin, A. C. B. M., Cardoso, A. C. F., Selistre-de-Araujo, H. S. and Cominetti, M. R. (2015). Recombinant disintegrin domain of human ADAM9 inhibits migration and invasion of DU145 prostate tumor cells. *Cell Adh. Migr.* **9**, 293-299.
- Mazzocca, A., Coppari, R., De Franco, R., Cho, J.-Y., Libermann, T. A., Pinzani, M. and Toker, A. (2005). A secreted form of ADAM9 promotes carcinoma invasion through tumor-stromal interactions. *Cancer Res.* **65**, 4728-4738.
- Miao, H., Burnett, E., Kinch, M., Simon, E. and Wang, B. (2000). Activation of EphA2 kinase suppresses integrin function and causes focal-adhesion-kinase dephosphorylation. *Nat. Cell Biol.* **2**, 62-69.
- Micocci, K. C., Martin, A. C., Montenegro, C. D. F., Durante, A. C., Pouliot, N., Cominetti, M. R. and Selistre-de-Araujo, H. S. (2013). ADAM9 silencing inhibits breast tumor cell invasion in vitro. *Biochimie* **95**, 1371-1378.
- Moss, M. L., Rasmussen, F. H., Nudelman, R., Dempsey, P. J. and Williams, J. (2010). Fluorescent substrates useful as high throughput screening tools for ADAM9. *Comb. Chem. High Throughput Screen.* **13**, 358-365.
- Nath, D., Slocombe, P. M., Webster, A., Stephens, P. E., Docherty, A. J. and Murphy, G. (2000). Meltrin gamma(ADAM-9) mediates cellular adhesion through alpha(6)beta(1)integrin, leading to a marked induction of fibroblast cell motility. *J. Cell Sci.* **113**, 2319-2328.
- Ni, H., Li, A., Simonsen, N. and Wilkins, J. A. (1998). Integrin activation by dithiothreitol or Mn2+ induces a ligand-occupied conformation and exposure of a novel NH2-terminal regulatory site on the beta1 integrin chain. *J. Biol. Chem.* **273**, 7981-7987.
- O'Shea, C., McKie, N., Buggy, Y., Duggan, C., Hill, A. D. K., McDermott, E., O'Higgins, N. and Duffy, M. J. (2003). Expression of ADAM-9 mRNA and protein in human breast cancer. *Int. J. Cancer* **105**, 754-761.
- Parsons, J. T., Horwitz, A. R. and Schwartz, M. A. (2010). Cell adhesion: integrating cytoskeletal dynamics and cellular tension. *Nat. Rev. Mol. Cell Biol.* **11**, 633-643.
- Paul, N. R., Jacquemet, G. and Caswell, P. T. (2015). Endocytic trafficking of integrins in cell migration. *Curr. Biol.* **25**, R1092-R1105.
- Peduto, L., Reuter, V. E., Shaffer, D. R., Scher, H. I. and Blobel, C. P. (2005). Critical function for ADAM9 in mouse prostate cancer. *Cancer Res.* **65**, 9312-9319.
- Pellegrin, S. and Mellor, H. (2007). Actin stress fibres. *J. Cell Sci.* **120**, 3491-3499.
- Ratcliffe, C. D. H., Sahgal, P., Parachoniak, C. A., Ivaska, J. and Park, M. (2016). Regulation of cell migration and beta1 integrin trafficking by the endosomal adaptor GGA3. *Traffic* **17**, 670-688.
- Roberts, M., Barry, S., Woods, A., van der Sluijs, P. and Norman, J. (2001). PDGF-regulated rab4-dependent recycling of alphavbeta3 integrin from early endosomes is necessary for cell adhesion and spreading. *Curr. Biol.* **11**, 1392-1402.
- Shattil, S. J., Kim, C. and Ginsberg, M. H. (2010). The final steps of integrin activation: the end game. *Nat. Rev. Mol. Cell Biol.* **11**, 288-300.
- Takeda, S., Takeya, H. and Iwanaga, S. (2012). Snake venom metalloproteinases: structure, function and relevance to the mammalian ADAM/ADAMTS family proteins. *Biochim. Biophys. Acta* **1824**, 164-176.
- Tao, K., Qian, N., Tang, Y., Ti, Z., Song, W., Cao, D. and Dou, K. (2010). Increased expression of a disintegrin and metalloprotease-9 in hepatocellular carcinoma: implications for tumor progression and prognosis. *Jpn. J. Clin. Oncol.* **40**, 645-651.
- Wang, F.-F., Wang, S., Xue, W.-H. and Cheng, J.-L. (2016). microRNA-590 suppresses the tumorigenesis and invasiveness of non-small cell lung cancer cells by targeting ADAM9. *Mol. Cell. Biochem.* **423**, 29-37.
- Weber, S. and Saftig, P. (2012). Ectodomain shedding and ADAMs in development. *Development* **139**, 3693-3709.
- Zhou, M., Graham, R., Russell, G. and Croucher, P. I. (2001). MDC-9 (ADAM-9/ Meltrin gamma) functions as an adhesion molecule by binding the alpha(v)beta(5) integrin. *Biochem. Biophys. Res. Commun.* **280**, 574-580.
- Zigrino, P., Nischt, R. and Mauch, C. (2011). The disintegrin-like and cysteine-rich domains of ADAM-9 mediate interactions between melanoma cells and fibroblasts. *J. Biol. Chem.* **286**, 6801-6807.
- Zubel, A., Flechtenmacher, C., Edler, L. and Alonso, A. (2009). Expression of ADAM9 in CIN3 lesions and squamous cell carcinomas of the cervix. *Gynecol. Oncol.* **114**, 332-336.



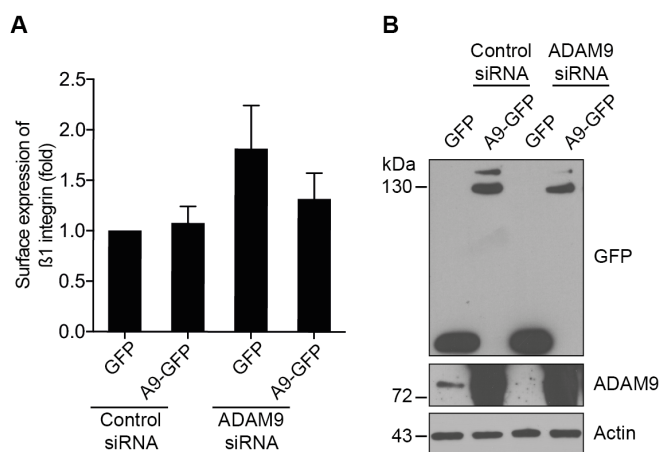
Supplementary figure S1: Confirmation of cell adhesion data in HT1080 cells

HT1080 cells were transfected with control or ADAM9 siRNA and 72 hours later serum starved o/n. Cells were plated on collagen I or fibronectin for 60 min and cell adhesion was measured calorimetrically. Adhesion to bovine serum albumin (BSA) was used as control and subtracted from the raw OD values. Data are shown as mean \pm standard error of the mean (SEM), for collagen I $n = 4$ and for fibronectin $n = 3$. * $p < 0.05$ as determined by Student's T-test.



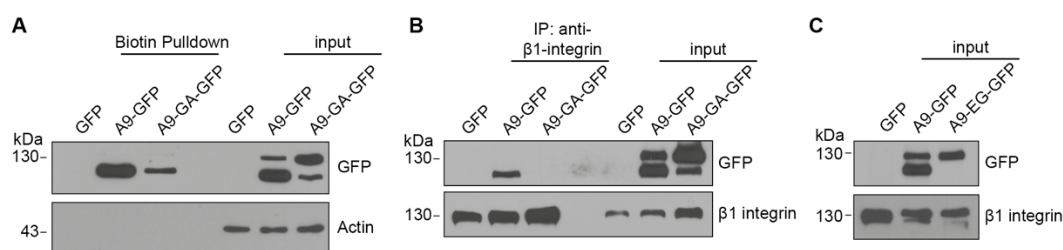
Supplementary figure S2: Knockdown of ADAM9 upregulated protein amount of $\beta 1$ integrin

PC3 (A, B, E, F) or HT1080 (C, D, G, H) cells were transfected with control or one of two different ADAM9 siRNAs and 72 hours later examined by Western blot (A-D) or qPCR (E-H) as indicated. The graphs in B and D show the quantification of Western blots in A and C, respectively. Actin was used as a loading control. Data are shown as mean \pm standard error of the mean (SEM), n = 3, except for D n = 4. *p < 0.05, ***p < 0.005 as determined by ANOVA.



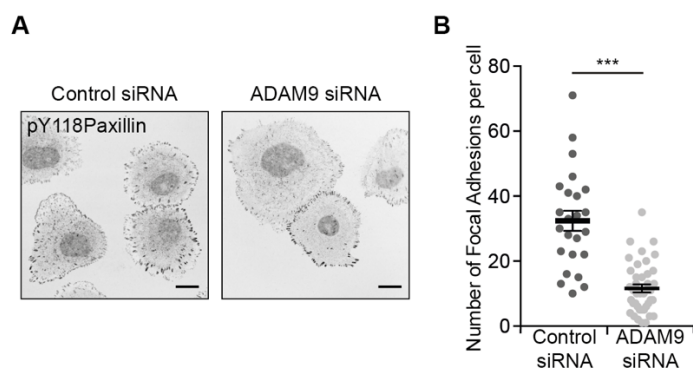
Supplementary figure S3: Expression of siRNA resistant ADAM9 in ADAM9-silenced cells

HT1080 cells were transfected with control or ADAM9 siRNA and 48 hours later transfected with empty GFP vector (GFP) or siRNA resistant murine ADAM9-GFP (A9-GFP). After additional 24 hours, the cells were (A) examined by flow cytometry for surface expression of $\beta 1$ integrin, and (B) examined by Western blot as indicated. Actin served as a loading control. Data are shown as mean \pm standard error of the mean (SEM), $n = 4$, and were analysed by ANOVA.



Supplementary figure S4: Mutation of the ADAM9 disintegrin domain

(A+B) HT1080 cells were transfected with empty GFP vector (GFP), wildtype ADAM9-GFP (A9-GFP) or the ADAM9 GA disintegrin mutant (ADAM9-GA-GFP). (A) Cells were surface biotinylated using non-cleavable, non-membrane permeable biotin, and biotinylated proteins were precipitated using streptavidin-agarose beads. Streptavidin and input samples were examined by Western blot. Actin served as a control. (B) Cells were lysed, immunoprecipitated with anti-β1 integrin antibody, and examined by Western blot. (C) HT1080 cells were transfected with empty GFP vector (GFP), wildtype ADAM9-GFP (A9-GFP) or the ADAM9 EG disintegrin mutant (ADAM9-EG-GFP), lysed and examined by Western blot.



Supplementary figure S5: Focal adhesion analysis

(A) PC3 cells were transfected with control or ADAM9 siRNA. Cells were serum starved o/n, plated on Collagen for 30 min and then fixed and stained for phosphorylated Paxillin (pY118Paxillin). (B) Quantification of the number of pY118Paxillin adhesions from A (3 independent experiments, 24 siControl and 41 siADAM9 cells analysed and individually plotted) Average values are indicated with a line. *** $p < 0.005$ as determined by Student's T-test.